Network-Wide Traffic States Imputation Using Self-interested Coalitional Learning

Huiling Qin[1,2], Xianyuan Zhan[2], Yuanxun Li[3], Xiaodu Yang[4], Yu Zheng[1,2]
[1]Xidian University, Xi'an, China
[2]JD Intelligent Cities Research, JD Technology, Beijing, China
[3]Sun Yat-sen University, Guangzhou, China
[4]Southwest Jiaotong University, Chengdu, China
{orekinana,zhanxianyuan}@gmail.com;liyx289@mail2.sysu.edu.cn;xiaodu.yang@foxmail.com;msyuzheng@outlook.com

ABSTRACT

Accurate network-wide traffic state estimation is vital to many transportation operations and urban applications. However, existing methods often suffer from the scalability issue when performing real-time inference at the city-level, or not robust enough under limited data. Currently, GPS trajectory data from probe vehicles has become a popular data source for many transportation applications. GPS trajectory data has large coverage area, which is ideal for network-wide applications, but also has the disadvantage of being sparse and highly heterogeneous among different time and locations. In this study, we focus on developing a robust and interpretable network-wide traffic state imputation framework using partially observed traffic information. We introduce a new learning strategy, called self-interested coalitional learning (SCL), which forges cooperation between a main self-interested semi-supervised learning task and a discriminator as a critic to facilitate main task training while providing interpretability on the results. In our detailed model, we use a temporal graph convolutional variational autoencoder (TG-VAE) as the reconstructor, which models the complex spatio-temporal pattern in data and solves the main traffic state imputation task. A discriminator is introduced to output interpretable imputation confidence on the estimated results and also help to enhance the performance of the reconstructor. The framework is evaluated using a large GPS trajectory dataset from taxis in Jinan, China. Extensive experiments against the state-of-the-art baselines demonstrate the effectiveness and robustness of the proposed method for network-wide traffic state estimation.

CCS CONCEPTS

• Computing methodologies → Learning paradigms; **• Theory of computation → Semi-supervised learning**.

KEYWORDS

Spatio-temporal data, Missing value imputation, self-interested coalition learning, temporal graph convolutional network

KDD '21, August 14–18, 2021, Virtual Event, Singapore

ACM ISBN 978-1-4503-8332-5/21/08…$15.00
https://doi.org/10.1145/3447548.3467424

ACM Reference Format:
Huiling Qin[1,2], Xianyuan Zhan[2], Yuanxun Li[3], Xiaodu Yang[4], Yu Zheng[1,2]. 2021. Network-Wide Traffic States Imputation Using Self-interested Coalitional Learning. In *Proceedings of the 27th ACM SIGKDD Conference on Knowledge Discovery and Data Mining (KDD '21), August 14–18, 2021, Virtual Event, Singapore.* ACM, New York, NY, USA, 9 pages. https://doi.org/10.1145/3447548.3467424

1 INTRODUCTION

Traffic state estimation at urban road network-level plays a central role in many transportation operations and applications. For example, local transportation agencies use real-time traffic state information for daily operation, such as traveler information provision, change timing configurations for certain traffic signals to alleviate congestion, and close certain roads on emergency events. Conventional traffic state information acquisition heavily relies on various road-based sensors, such as loop detectors or traffic monitoring cameras. This requires installing a large number of sensors, which is neither cost-effective nor practical for city-scale monitoring. Thus these approaches are mainly applied to major roads or limited-scale road networks. The recently emerged crowd-based mobile sensing data, such as the trajectory data from GPS unit installed taxis or cellphones, provide a new alternative for collecting

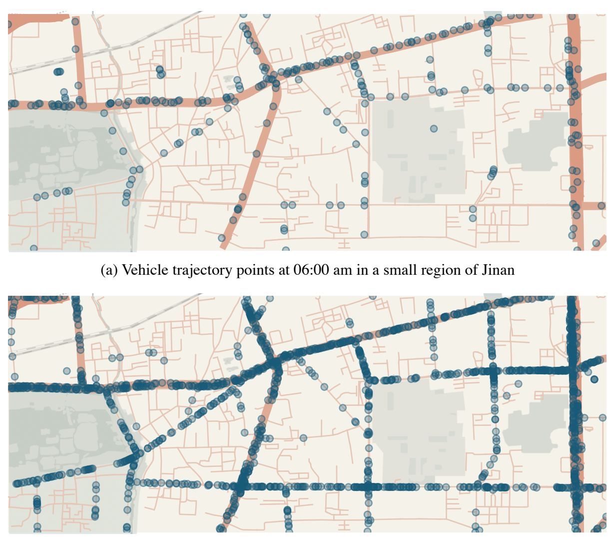

(a) Vehicle trajectory points at 06:00 am in a small region of Jinan

(b) Vehicle trajectory points at 17:00 am in a small region of Jinan

Figure 1: Spatio-temporal heterogeneity in trajectory data

and utilizing network-wide traffic state information. However, accurately estimating network-wide traffic state from large-scale mobile sensing data is still a difficult task involving many challenges:

- **Data Sparsity.** As probe vehicles such as taxis only account for a small fraction of the total traffic, which induce a very sparse and partially monitored the road network [29]. This situation can be even worse during off-peak hours when the number of probe vehicles in the road network is small.
- **Complex spaio-temporal pattern.** The traffic conditions of the road network are strongly influenced by the rhythm of the city as well as human urban activity and mobility patterns [15]. For instance, congestion in rush hours and free-flow in off-peak hours. These lead to highly heterogeneous spatio-temporal patterns in the vehicle trajectory data (see Figure 1 as an example) and greatly increase the difficulty of imputing unknown traffic states based on the underlying dynamics from the partially observed data.
- **Data unreliability.** As the raw traffic states information, such as road speeds, are obtained from sample vehicle trajectories. Even the directly observed traffic states may not be reliable or have high variance under the impact of drivers' different driving behaviors, sampling bias and data sparsity.
- **Interpretability.** Given the reliability and high variance issue in the partially observed data, it is desired to have a model making traffic state imputation together with certain level of interpretability, such as estimation confidence of both the observed and imputed data. Most of the existing models fully trust the input data and lacks interpretability of the results [1, 21, 28, 30, 31], which could lead to less robust transportation applications.
- **Real-time inference.** Real-world transportation applications typically require updating traffic state information for large road network as frequently as possible. It needs to have an efficient and easy-to-deploy model to meet the real-time requirements.

To address the aforementioned challenges, we propose a new Spatio-Temporal Self-interested Coalitional Learning framework (ST-SCL) to solve the network-wide traffic state imputation problem given partially observed data. In particular, we focus on robustly imputing unknown road speeds while simultaneously providing estimated confidence on both imputed and observed road speeds.

The self-interested coalitional learning (SCL) is a novel strategy that enhances the performance of a semi-supervised learning task by introducing an additional discriminator and forges cooperation between these two tasks to boost their performance. In our problem, we use a reconstructor to solve the main traffic state imputation problem. An additional discriminator is learned as a critic to output confidence values and judge whether data samples are reliable or not with the help of extra information (i.e. reconstruction error) provided by the reconstructor. The reconstructor also uses the judgment from the discriminator to boost its own performance, while being self-interested that tries to challenge the discriminator by providing as little information as possible. SCL is different from the ideas of multi-task learning [18] and adversarial learning [7]. In SCL, the two tasks are neither fully cooperative as in multi-task learning, nor fully adversarial to each other as in adversarial learning, but balance the benefit of cooperation and competition.

For the detailed modeling for our traffic state imputation problem, we construct a temporal graph convolutional variational autoencoder (TG-VAE) as the reconstructor to capture the spatio-temporal dependency in the dynamic traffic state data and perform missing state imputation. The discriminator uses a similar encoder structure as in the reconstructor with additional reconstruction errors as input, and provides estimated confidence values of the data.

Our main contributions are summarized as follows:

- We propose the ST-SCL, a new framework that performs real-time network-wide traffic state imputation with partially observed input data, while providing interpretable confidence on the results.
- We develop a novel self-interested coalitional learning (SCL) strategy that can boost the performance of a semi-supervised learning task by forging cooperation with an extra discriminator in a self-interested manner. SCL has three major advantages over multi-task and adversarial learning: 1) It achieves superior performance compared with the multi-task and adversarial learning version of the problem in empirical experiments. 2) It naturally provides the data confidence measures from the discriminator as a byproduct of the learning process, which can offer additional interpretability for the main task. 3) SCL is very easy to train in contrast to the notable training difficulty in GAN.
- We design a highly customized reconstructor and discriminator for the traffic state imputation problem, which captures both the complex spatio-temporal traffic dynamics as well as the dependency structure of the road network using sparse, noisy and partially observed traffic state data.
- We conduct extensive experiments using a large real-world taxi trajectory dataset. The results show that the proposed ST-SCL consistently achieves superior imputation accuracy over all the state-of-the-art baseline methods in different cases, with the additional capability of providing confidence measures on the results. Experiments also show that ST-SCL is robust under different missing rates compared with its variants and baseline methods. These demonstrate the effectiveness of the proposed ST-SCL framework for the network-wide traffic state imputation problem.

2 PRELIMINARIES

Definition 2.1. **Road adjacency graph.** To model the road-based traffic states, we consider the road network as a graph $G = \{R, A\}$, where roads are considered as the nodes R in graph G, and A is the adjacency matrix representing the connectivity between roads.

Definition 2.2. **Trajectory.** A trajectory is a sequence of spatio-temporal points, denoted as $tr =< p_1, p_2, \cdots, p_n >$, where each point $p = (x, y, t)$ consists of a location (x, y) (i.e., longitude and latitude) at time t. Points in a trajectory are organized chronologically, that is $\forall i < j, p_i.t < p_j.t$.

Definition 2.3. **Partially observed traffic state data.** We denote X as the traffic speed data extracted from vehicle trajectories on the road network G. Let x_t^r be the speed of road $r \in R$ at time step t, and we write the traffic speeds for all roads in R over the time period $[t_0 : t_n]$ as a matrix $X_{t_0:t_n} = \left[x_{t_0:t_n}^r | r \in R\right]$. We similarly write the number of trajectories on the roads as $S_{t_0:t_n} = \left[s_{t_0:t_n}^r | r \in R\right]$, in which s_t^r is the trajectory support of road r at time step t. As the trajectory data only sparsely cover the road network at a time step, X is partially filled. For ease of later modeling process, we compute the mean μ^r of the observed speeds during $[t_0 : t_n]$ for each road r, and fill the missing entries in X with μ^r adding a random noise.

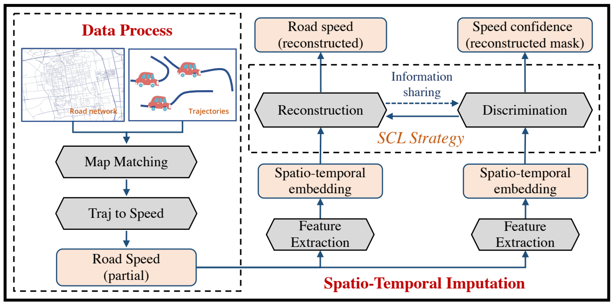

Figure 2: Overall framework

Definition 2.4. **Observability Mask.** We define a mask matrix M, with $M_{t_0:t_n} = \left[m^r_{t_0:t_n} | r \in R\right]$ denoting the observability of traffic states over the time period $[t_0 : t_n]$. We set $m^r_t = 1$ if x^r_t is observed ($s^r_t > 0$), and $m^r_t = 0$ if x^r_t is missing ($s^r_t = 0$). For simplicity, we also introduce sets O and U to denote the set of observed and unobserved entries of X (i.e. $x^r_t \in O$ if $m^r_t = 1$; $x^r_t \in U$ otherwise).

Our goal is to reliably impute all the missing entries (initially randomly filled) in road speeds data $X_{t_0:t_n}$ by constructing a filled matrix $\hat{X}_{t_0:t_n}$ of a given road network G and time interval $[t_0 : t_n]$, while providing the imputation confidence $P_{t_0:t_n} = \left[p^r_{t_0:t_n} | r \in R\right]$ of the results (equivalent to the reconstruction of M for both observed and imputed values). We denote our traffic state imputation task as a mapping: $\mathcal{F}(X, M) \mapsto [\hat{X}, P]$.

3 OVERALL FRAMEWORK

In this section, we introduce the data processing process and an overview for the spatio-temporal traffic state imputation modeling process. Figure. 2 shows the overall framework of this paper.

Data processing. We use a hidden Markov model (HMM) based map matching technique [26] to map the points of a trajectory $Tr =< tr_1, tr_2, \cdots, tr_n >$ to a sequence of roads $r_1 \rightarrow r_2 \rightarrow \cdots \rightarrow r_n$ given the road network. Based on the map-matched trajectories, we calculate the distance and time elapse between consecutive trajectory points, and compute their divided value as the speed at each point. By aggregating all the speeds of trajectories on a road r within a time step t, we obtain the real-time speed x^r_t of the road. For overly large travel speeds (possibly belong to speeding vehicles), we reset the speeds to the speed limit of the road.

Spatio-temporal imputation. Based on the extracted partially observed speeds, we propose a self-interested coalitional learning strategy that leverages a reconstructor to solve the traffic state imputation task, and a discriminator to provide interpretable confidence measures on the results. SCL forges cooperation through information sharing between the reconstructor and discriminator to boost their performance. We introduce a Temporal Graph Convolutional Variational Autoencoder (TG-VAE) as the reconstructor. It extracts and utilizes the spatio-temporal embedding of data and infers the missing road speeds by reconstructing the partially observed data. A Mask Discriminative Network (MDN) is modeled as the discriminator. It accepts additional information from the reconstructor and provides confidence measures of the imputed results by reconstructing the observability mask of the data.

4 SELF-INTERESTED COALITIONAL LEARNING

Our traffic state imputation problem can be abstracted as simultaneously solving two tasks. The main task uses a reconstructor f with generative capacity to impute complete data $\hat{X}$ from partially observed data X. The other task uses a discriminator d to provide interpretable confidence measures P by reconstructing the original observability mask M using information from both X and $\hat{X}$. As the randomly filled unobserved entries in X may have different patterns compared with normal data. One can expect larger difference between X and the reconstructed $\hat{X}$ at unobserved entries, which provides clues for the discriminator d to judge their observability. This design also allows the discriminator to detect unreliable observed data (e.g. high variance road speeds caused by sampling bias and data sparsity of vehicle trajectories), as they also possess different patterns against normal data, which are more likely to be considered as unobserved by the discriminator.

These two tasks can be formally formulate as follows:

$$\begin{aligned} A &: f(X) = \hat{X}, \qquad \mathcal{L}_A = loss_A(X, \hat{X}) \\ B &: d(X, \hat{X}) = P, \quad \mathcal{L}_B = loss_B(P, M) \end{aligned} \tag{1}$$

where Task A essentially can be any semi-supervised learning task with $\hat{X}$ being replaced to the target labels $\hat{Y}$ predicted based on the partially observed data X. $loss_A$ and $loss_B$ can be any loss functions for semi-supervised and discriminative tasks. For example, the commonly used mean square error (MSE) can be used in $loss_A$ for data reconstruction, and binary cross entropy (BCE) loss can be used in $loss_B$ for discriminating sample observability. In our traffic state imputation problem, Task A is a data reconstruction task, and we only compute the loss for the observed entries ($x_i \in O$).

4.1 Conventional approaches

As the two tasks defined in Eq.1 need to be jointly solved, a straightforward approach is through a multi-task learning style multi-objective optimization method to exploit the shared information and underlying commonalities between the two tasks. This can be achieved by minimizing the following combined loss:

$$\min_{f,d} \lambda \cdot loss_A + (1 - \lambda) \cdot loss_B, \quad \lambda \in (0, 1) \tag{2}$$

However, there are two downsides for this treatment. First, the reconstructor f and discriminator d solve different tasks. There could be some potential contradictions of the two tasks in certain settings, where jointly minimizing the augmented loss function may impede both tasks from achieving the best performance. Second, tuning the additional weight hyperparameter λ can be tricky.

Another approach is to use the adversarial learning such as GAN [7], which makes the generator (in our case is the reconstructor) and discriminator learn against each other, thus improves the performance of both tasks. The optimization objective is

$$\min_{f} \max_{d} M \odot \log d(X, f(X)) + (1 - M) \odot \log(1 - d(X, f(X))) \tag{3}$$

where $\odot$ is the Hadamard product. Under the adversarial learning framework, $loss_A$ is not explicitly optimized. The training of the main task f completely depends on the outputs of the discriminator d, which results in potential loss of information. Moreover solving

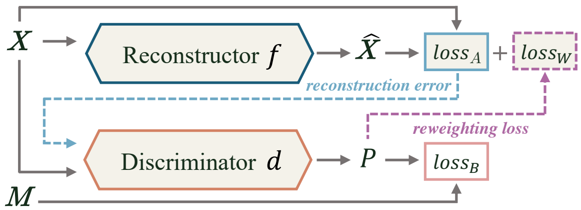

Figure 3: Illustration of the SCL strategy

the above minimax optimization problem is much harder compared with directly minimizing $loss_A$ in a supervised learning fashion, which causes GAN-style models notoriously hard to train.

4.2 An improved strategy: SCL

We propose a new learning scheme to solve the two tasks in Eq.1, called self-interested coalitional learning (SCL). We modify the loss of Task A $\mathcal{L}_A$ as well as the inputs of Task B into following form:

$$\begin{aligned} &A: f(X)=\hat{X}, && \mathcal{L}_A = loss_A(X,\hat{X}) + loss_W(X,P) \\ &B: d(X, g(X,\hat{X}))=P, && \mathcal{L}_B = loss_B(P,M). \end{aligned} \tag{4}$$

As illustrated in Figure 3, in SCL, the two tasks are neither fully cooperative as in multi-objective optimization, nor fully adversarial to each other as in adversarial learning, but balance the benefit of cooperation and competition. The reconstructor f uses the information from the discriminator d (output confidence measures P) to facilitate its learning by introducing an additional loss term $loss_W(X,P)$. At the same time, the reconstructor f also provide extra reconstruction error information to discriminator d encoded in $g(X,\hat{X})$. Both parties use information from each other to improve their own task performance. Moreover, we consider the reconstructor f being self-interested that tries to challenge the discriminator by providing as little information in $g(X,\hat{X})$ as possible. This can be considered as a coalitional game with one part being self-interested. During the cooperative process, when reconstruction error $g(X,\hat{X})$ no longer provides useful information for the judgment of the discriminator d, then we may have reason to believe the reconstructor f has achieved satisfactory data reconstruction performance.

In our traffic state imputation problem, we consider MSE and BCE loss as $loss_A$ and $loss_B$ for the two tasks. We defined $g(X,\hat{X}) = (X-\hat{X})^2$, which is the element-wise squared error between input X and reconstructed data $\hat{X}$. The derivative of d, h_B is given as:

$$h_B = \frac{\partial \mathcal{L}_B}{\partial d} \quad = -\sum \left[M \oslash d(X, g(X, f(X))) - (1-M) \oslash (1 - d(X, f(X)) \right]$$

where $\oslash$ is the Hadamard division. We are interested to see how the variation of f impacts the information provided in h_B by calculating its derivative:

$$\begin{aligned} &\frac{\partial h_B}{\partial f} = \frac{\partial h_B}{\partial g} \cdot \frac{\partial g}{\partial f} \\ &= -\sum \left[M \oslash d(X, g(X, f(X))) - (1-M) \oslash (1 - d(X, f(X)) \right] \\ &\odot 2(X - f(X)) \odot \nabla f(X) \\ &= -\sum_{x_i \in O} \frac{2}{p_i}(x_i - \hat{x}_i) \cdot \nabla f(x_i) + \sum_{x_j \in U} \frac{2}{1-p_j}(x_i - \hat{x}_i) \cdot \nabla f(x_j) \end{aligned} \tag{5}$$

For convenience, we write p_i as the ith entry of $d(X, g(X, f(X)))$ in the last line of Eq.5. Note that $2(X - f(X)) \cdot \nabla f(X)$ is the gradient of squared reconstruction error $(X - f(X))^2$ with respect to f, hence the result of Eq.5 can be equivalently perceived as the gradient of a new term $L_f(X,P)$ ($\partial h_B / \partial f = \partial L_f / \partial f$) with following form:

$$L_f(X,P) = -\sum_{x_i \in O} \frac{1}{p_i} \cdot (x_i - \hat{x}_i)^2 + \sum_{x_j \in U} \frac{1}{1-p_j} \cdot (x_j - \hat{x}_j)^2 \tag{6}$$

As reducing the amount of information provided by the constructor f for discriminator d is essentially driving the gradient $\partial h_B / \partial f \to 0$. Eq.5-6 indicate that this can be achieved by finding the local minimum or maximum of $L_f(X,P)$ with respect to f. In both cases, we can achieve $\partial h_B / \partial f = \partial L_f / \partial f \to 0$. However, it can be observed that minimizing $L_f(X,P)$ is not a feasible option, as it will increase the reconstruction errors $(x - \hat{x})^2$ for observed samples and decrease the reconstruction errors for unobserved samples, which contradicts with the purpose of the reconstructor. Hence we maximize the $L_f(X,P)$ by introducing an additional loss term $loss_W(X,P) = -L_f(X,P)$ in $\mathcal{L}_A$ as follows:

$$loss_W(X,P) = \sum_{x_i \in O} \frac{1}{p_i} \cdot (x_i - \hat{x}_i)^2 - \sum_{x_j \in U} \frac{1}{1-p_j} \cdot (x_j - \hat{x}_j)^2 \tag{7}$$

We now obtain the exact form of $loss_W$ described in SCL scheme (Eq.4) under $loss_B$ being BCE loss. $loss_W$ can be considered as additional reweighting loss that complements the original loss term $loss_A$ based on the estimated confidence P from discriminator d.

4.3 Interpretation of SCL

Adding $loss_W$ to the original loss term $loss_A$, we can obtain the complete loss for the main reconstruction task A as:

$$\mathcal{L}_A = \sum_{x_i \in O} (1 + \frac{1}{p_i}) \cdot (x_i - \hat{x}_i)^2 - \sum_{x_j \in U} \frac{1}{1-p_j} \cdot (x_j - \hat{x}_j)^2 \tag{8}$$

This essentially transforms the original main task into a cost-sensitive learning problem [27] by imposing following re-weighting factors on the squared errors of each element x_i as:

$$\text{Re-weighting factor} = \begin{cases} 1 + 1/p_i, & x_i \in O \\ -1/(1-p_j), & x_j \in U \end{cases} \tag{9}$$

Above re-weighting factors induce very different behaviors on the reconstruction errors $(x - \hat{x})^2$ of observed and unobserved entries of X. As p_i represents the judgment of the discriminator d on whether x_i is observed or not. For observed entries, the reconstruction errors are boosted by additional weight of $1/p_i$. Note that if discriminator d judges an observed entry $x_i \in O$ to be unobserved or unreliable (confidence $p_i \to 0$), the reconstruction error of this entry will get significantly boosted. This forces the reconstructor f to pay more attention to reconstructing the problematic observed entries. As unobserved entries $x_j \in U$ in X are initially filled with random values, well imputed entries $\hat{x}_j$ ideally should keep a reasonably large reconstruction error $(x_j - \hat{x}_j)^2$. For unobserved entries, the discriminator d encourages the reconstructor f to enlarge the reconstruction error on these entries by a factor of $1/(1-p_j)$. Specifically, the more likely an entry x_j is considered reliable by the discriminator ($p_j \to 1$), the stronger it forces the reconstructor to ignore further improvement on imputing x_j.

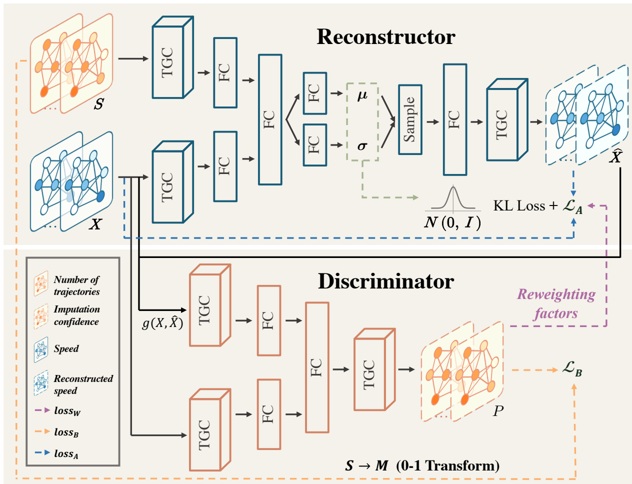

Figure 4: Detailed ST-SCL model design for our problem

The form of re-weighting factors in Eq.9 are derived with MSE and BCE losses for $loss_A$ and $loss_B$, and $g(X, \hat{X}) = (X - \hat{X})^2$. SCL provides a very flexible framework. Different semi-supervised learning task and discrimination task with other choices of $loss_A$, $loss_B$ and g could also lead to different forms of re-weighting factors. As the re-weighting factors in Eq.9 can potentially have infinite values, in practical implementation, we clip the factors to $[-10, 10]$.

5 DETAILED MODEL CONSTRUCTION

Based on the previously developed SCL strategy, we introduce a spatio-temporal reconstructor and a mask discriminative network (MDN) as the discriminator to solve the traffic state imputation problem. We specifically consider and model the spatio-temporal traffic dynamics and the underlying data dependency imposed by the road network, detailed model design is presented in Figure 4.

5.1 Spatio-temporal reconstruction

The underlying road network structure could induce a strong correlation for traffic speeds on adjacent roads. To better model the temporal traffic dynamics pattern as well as the dependency structure across roads, we design a temporal graph convolutional variational autoencoder (TG-VAE) as the reconstructor for speed data reconstruction. TG-VAE is a combination of a Temporal Graph Convolutional (TGC) network [22] and a Variational Auto-Encoder (VAE) [9] (see Figure. 4).

In our TGC network, a temporal convolutional layer first applies 1-D convolution filters on the time dimension of the input road speed data X and trajectory support S to extract high-level temporal embeddings Y_X, Y_S for each road. A graph convolutional network (GCN) layer is then used to further capture the structural dependency in the extracted temporal data embeddings according to road network structure. We use the GCN layer proposed in Defferrard et al. [3] that considers a spectral convolution on graph defined as the multiplication of a graph signal Y with a filter J_θ parameterized by θ in the Fourier domain. In order to enable fast evaluation, We used the Kth-order polynomial in the Laplacian, which restricts the GCN to capture the information at maximum K steps away from the central node (K-localized, $K = 2$ in our implementation). The corresponding graph convolutional operator and the lth layer output of GCN $H^{(l)}$ given activation function $act(\cdot)$ are as follows:

$$J_\theta(L)Y = \sum_{k=0}^{K-1} \theta_k L^k Y, \quad H^{(l+1)} = act\Big(\sum_{k=0}^{K-1} \theta_k L^k H^{(l)}\Big)$$

where L is the normalized graph Laplacian of the road adjacency matrix A. TGC network play a key role in our TG-VAE model design, which extracts spatio-temporal embeddings of the data and greatly improves the data reconstruction capability.

In the encoder of TG-VAE, the spatio-temporal embeddings extracted by TGC networks from the speed data X and trajectory support S are fused using fully connected (FC) layers. They jointly generate a latent vector z that roughly follow a Gaussian distribution $N(\mu, \sigma)$. Finally, TG-VAE outputs the filled traffic speed data $\hat{X}$ using a decoder that is modeled as an FC layer followed by a TGC network. Based on the SCL strategy in the previous section, we train the proposed TG-VAE reconstructor by minimizing the following evidence lower bound (ELBO) objective function:

$$\min_f \mathcal{L}_A + \lambda_f \cdot \sum_i KL[q_\theta(z_i|X_i, P_i)||N(\mathbf{0}, \boldsymbol{I})] \tag{10}$$

where $\mathcal{L}_A$ is the reconstruction loss defined in Eq.8 and λ_f is a weight parameter. The KL divergence $KL[q_\theta(z_i|X_i, P_i)||N(\mathbf{0}, \boldsymbol{I})$ forces the posterior distribution $q_\theta(z_t|X_t, P_t)$ approximated by the encoder of TG-VAE to be similar to the prior distribution $N(\mathbf{0}, \boldsymbol{I})$.

5.2 Mask discriminative network

The unobserved speeds in the traffic speed data X are initially filled with random data. They can be considered as anomalies that have different patterns compared with the normal data, and harder to reconstruct based on the learned patterns of normal data [16, 32]. Inspired by this observation, we introduce a mask discriminative network (MDN) as the discriminator d. MDN shares a similar architecture as the encoder of the reconstructor, but takes the inputs of the speed data X and the element-wise squared reconstruction errors $(X - \hat{X})^2$ from the reconstructor. This generates a feature embedding that is then used to output the final speed confidence estimates P through a TGC network followed by a sigmoid activation layer. The training of MDN is achieved by minimizing the BCE loss $\mathcal{L}_B$ between the observability mask M and the estimated speed confidence measures P as discussed in Eq.4.

5.3 Implementation design

In our ST-SCL framework, the data flow is slightly different between the training stage and the online serving stage (see Figure 5). In

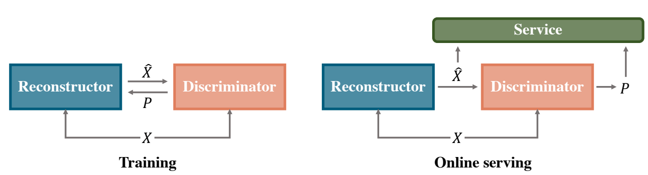

Figure 5: Training and online serving stages in ST-SCL

Table 1: Evaluation results of ST-SCL and the baseline methods for morning and evening peak, flat peak, and night hours

Methods	Overall		Morning peak		Evening peak		Flat peak		Night hour	
	MSE	RMSE	MSE	RMSE	MSE	RMSE	MSE	RMSE	MSE	RMSE
GAIN	0.1035	0.3217	0.0993	0.3151	0.0889	0.2982	0.0886	0.2977	0.2095	0.4577
MIWAE	0.1053	0.3245	0.1065	0.3263	0.1114	0.3338	0.1018	0.3191	0.0983	0.3135
MCFlow	0.0751	0.2740	0.0807	0.2841	0.0761	0.2759	0.0726	0.2694	0.0773	0.2780
MF	0.1314	0.3625	0.1326	0.3641	0.1186	0.3444	0.1182	0.3438	0.2295	0.4791
ST-SCL	**0.0679**	**0.2605**	**0.0740**	**0.2720**	**0.0697**	**0.2640**	**0.0677**	**0.2601**	**0.0617**	**0.2483**
ST-SCL-M	0.0703	0.2651	0.0752	0.2742	0.0718	0.2680	0.0683	0.2613	0.0725	0.2693
ST-SCL-G	0.1518	0.3896	0.1486	0.3854	0.1469	0.3832	0.1511	0.3887	0.1612	0.4014
ST-SCL(-D)	0.0683	0.2613	0.0747	0.2733	0.0704	0.2653	0.0678	0.2603	0.0622	0.2493
ST-SCL(-V)	0.0695	0.2636	0.0754	0.2746	0.0724	0.2691	0.0695	0.2636	0.0631	0.2512

the training stage, the discriminator uses the original traffic speeds X and the element-wise reconstruction error $(X - \hat{X})^2$ from the reconstructor as inputs ($P = d(X, (X - \hat{X})^2)$). The information of the reconstructed data $\hat{X}$ and the estimated speed confidence P of X are shared between the two models for each gradient update during training. The training updates of reconstructor and discriminator are applied simultaneously until both models converge.

While in the online serving stage, the discriminator uses the reconstructed road speeds $\hat{X}$ and the element-wise reconstruction error $(X - \hat{X})^2$ from the reconstructor as inputs ($P = d(\hat{X}, (X - \hat{X})^2)$). This generates the estimated speed confidence P for the reconstructed road speeds $\hat{X}$, which can be used to evaluate the reliability of both the unobserved and the observed road speeds.

6 EXPERIMENTS

In this section, we present the detailed evaluation of the proposed ST-SCL framework on a large taxi trajectory dataset and demonstrate its effectiveness against other competing baselines.

6.1 Datasets

Road network. The road network from the central region of Jinan, China is used in this study. It comprises 2938 nodes and 4033 edges. After filtering some low-level road segments (speed limit lower than 30km/h), we obtain a network with 608 road segments.

GPS trajectories. We use a GPS trajectory dataset generated by 33,851 Jinan taxis over a period of 30 days. The average sampling rate is 3 seconds per point. We set the time step length as 5 minutes for our problem. After projecting the trajectories on the road network, we obtain the average missing rate (proportion of unobserved road segments) for different time periods as shown in Table 2.

Table 2: Partition of time periods and related missing rates

Time period	All day	Morning peak	Evening peak	Flat peak	Night hour
Time	00:00-24:00	06:00-10:00	10:00-18:00	18:00-20:00	20:00-06:00
Missing rate	37.9%	15.4%	17.1%	27.0%	77.2%

Settings. We partition the traffic speed data into a 28-day training set and a 2-day testing set for model evaluation. We use the mean square error (MSE) and root mean square error (RMSE) to evaluate the performance of the proposed model.

6.2 Baselines

We consider several state-of-the-art imputation approaches and a few widely used spatio-temporal methods as baselines:

- **GAIN.** Generative Adversarial Imputation Nets (GAIN) [25] generalizes the GAN [7] to operate in partially observed data. In GAIN, the generator's goal is to accurately impute missing data, and the discriminator's goal is to distinguish between observed and imputed components.
- **MIWAE.** Mattei et al. [11] consider the problem of handling missing data with deep latent variable models (DLVMs). It is based on the importance-weighted autoencoder (IWAE), which maximizes a potentially tighter lower bound of the log-likelihood.
- **MCFlow.** Richardson et al. [17] propose MCFlow, a deep framework for imputation that leverages normalizing flow generative models and Monte-Carlo sampling. It addresses the causality dilemma that arises when training models with incomplete data by introducing an iterative learning strategy.
- **MF.** Matrix factorization [8] decomposes a matrix with missing values into multiple low-rank matrices to uncover the latent features in data. The decomposed matrices are multiplied to obtain a fully filled matrix to impute the missing entities.
- **Variants of ST-SCL.** We compare multiple variants of ST-SCL to fully evaluate its performance, including: (1) **ST-SCL(-D)**: we drop the discriminator component to evaluate the effectiveness of SCL; (2) **ST-SCL(-V)**: the temporal graph convolution (TGC) layers are removed to test the impact of spatio-temporal modeling for the traffic data; (3) **ST-SCL-M**: the reconstructor and discriminator are learned using the multi-objective optimization approach as in Eq.2; (4) **ST-SCL-G**: the reconstructor and discriminator are learned using the generative adversary strategy as in Eq.3 to validate the performance of SCL.

6.3 Evaluation

Imputation accuracy. We compared our model with baselines in four representative time periods (see Table 2 for time periods partition) of a day to demonstrate the performance of traffic state imputation in different situations. To make a fair comparison, we present in Table 1 the best performance of each method under fine-tuned parameter settings. ST-SCL achieves superior performance over all baselines in both peak and off-peak time periods, with improvements of at least 5% to 10% on RMSE and MSE. Moreover, although more dynamic traffic patterns and diverse driving behaviors during rush hours cause large variance in traffic speeds, ST-SCL still maintains an RMSE of approximately 30% lower than the baselines. These results suggest that ST-SCL is effective and robust, especially in complex spatio-temporal scenarios.

The data sparsity issue during night hours poses great challenge of accurate imputation for most baseline methods. MF performs badly at almost all time periods because of its limited capability to handle sparse data and poor generalization ability. As the learning of the generator in GAN relies on the gradient backpropagation of the discriminator's loss function, the performance of GAIN is heavily impacted by the capability of its discriminator. The data at nighttime can be overly sparse for the discriminator to make correct judgement, which results in low imputation accuracy for GAIN in these time periods. MCFlow and MIWAE use probability density modeling to enhance the robustness of the model. However, it is still difficult to capture the correct data distribution under very unbalanced and sparse data regions. The proposed ST-SCL provides better expressiveness as well as additional explanatory information to differentiate the relative importance of learning on different data samples, which results in superior performance.

To further investigate the effectiveness of ST-SCL, we compare the performance of ST-SCL with its variants in Table 1. It is observed that the accuracy of ST-SCL(-D) is lower than that of ST-SCL due to the lack of useful information provided by the discriminator. ST-SCL-M jointly models the reconstruction and discriminating tasks, which weakens the accuracy of the reconstruction task due to potential contradictions of the two tasks in certain settings. ST-SCL-G models the two tasks in an adversarial learning setting similar to GAN. However, optimizing the reconstruction task through the discriminator loses the useful reconstruction loss information and leads to inferior imputation performance. Finally, from the comparison of ST-SCL and ST-SCL(-V), we observe that modeling the spatio-temporal correlation in the data also plays an important role in improving the model performance.

Robustness under different missing rates. To further evaluate the robustness of ST-SCL, we selected three baselines (MCFlow, MIWAE, GAIN) and two variants (ST-SCL-M, ST-STL-(D)) that perform well in previous evaluation for comparison. By randomly replacing some of the original data with random noise, we gradually increased the missing rate of the dataset from 40% (original missing rate 37.9%) to 70%. The results are shown in Figure 6.

Figure 6(a) shows that most of the baselines have unsatisfactory performance under increased missing rates. The Monte-Carlo based generative properties in MCFlow allows it to maintain relatively stable accuracy at missing rates below 70%, but the imputation error rises sharply when the missing rate reaches 70%. In terms of the variants, due to explicitly modeling of the spatial-temporal dependence in data, their imputation errors increase slowly when missing rates below 70%. However, when the missing rate reaches 70%, the error of the variants increase as sharply as the baseline methods. The comparison against ST-SCL-G is not included as its imputation error is more than twice that of ST-SCL at different missing rate. ST-SCL performs cost-sensitive learning for different

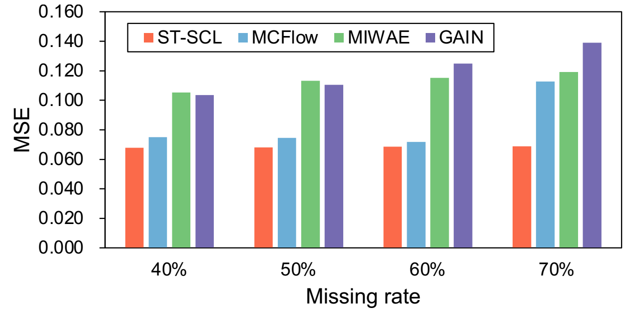

(a) The performance of ST-SCL and baselines under different missing rate

(b) The performance of ST-SCL and its variants under different missing rate

Figure 6: The performance under different missing rate

data samples, which lead to more stable and accurate imputation performance under different missing rates.

Interpretability of the ST-SCL. It is well-known that when the number of trajectories covering a road is limited, the sampled speeds will be unreliable and may deviate from historical averages. To validate this property, we plot the original speeds in data and the corresponding historical mean values under different number of trajectories supports s. Figure 7(a)(I) shows the case that only one trajectory covering a road ($s = 1$, low confidence), the original speeds deviate significantly from the historical means. While Figure 7(a)(II) shows that the original speeds on roads with higher trajectory support ($s > 2$, high confidence) are more similar to their historical means. Figures 7(a)(III), (IV) show the reconstruction results of ST-SCL with different imputation confidence levels p. For road speeds with $p > 0.5$, the reconstructed speeds are very similar to historical averages as well as the pattern in 7(a)(II). For road speeds with $p < 0.5$, ST-SCL corrects the original noisy speeds and provides reconstructed values that are closer to historical means.

Meanwhile, to evaluate the judgement of the discriminator, we analyze the trajectory supports of road speeds with $p < 0.5$. In Figure 7(b), most road speeds with low confidence ($p < 0.5$) identified by the discriminator are not covered by any trajectory. A number of road speeds covered by 1-2 trajectories are also identified as low confidence samples due to unreliable speed data. Besides, from the subplot in Figure 7(b), we see that the road speeds covered by limited trajectories differ greatly from their historical mean. This also indicates the unreliability of speeds on these roads. These analyses demonstrate the effectiveness of the discriminator in judging missing and unreliable data.

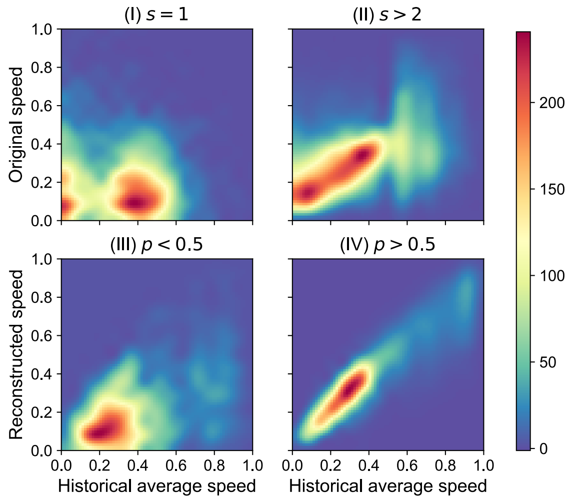

(a) Heatmap of normalized historical average and original/reconstructed speeds

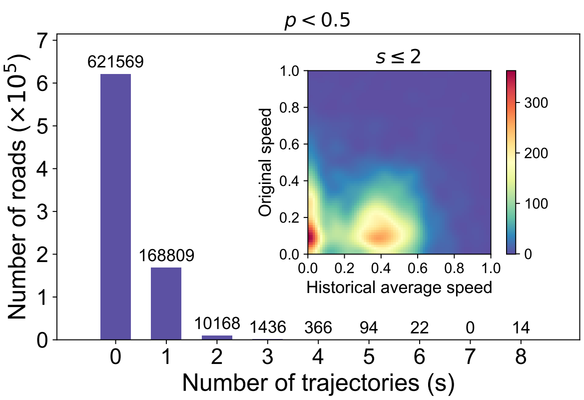

(b) Analysis on trajectory supports of road speeds with p < 0.5

Figure 7: Relationships of normalized historical average and original/reconstructed speeds under different trajectory supports and confidence levels.

(a) Historical average speed

(b) Original speed

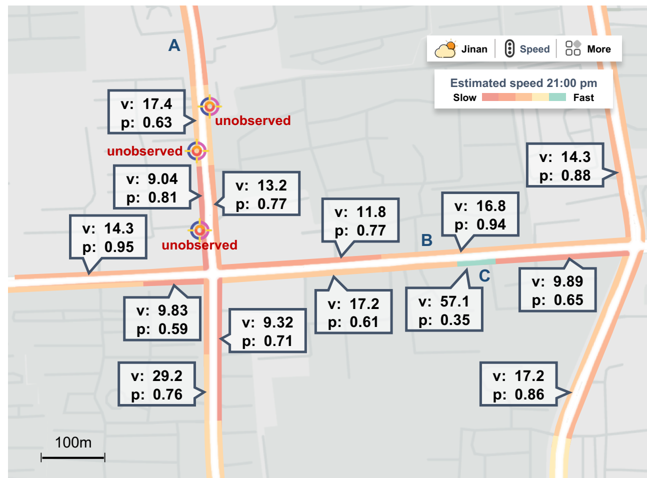

(c) Estimated speed

Figure 8: Comparison among historical average, original, and estimated speeds in Jinan at 2017/09/02 21:00.

Case study. A real-world example is visualized in Figure 8, showing the speed imputation results in a small region of Jinan at 21:00. Figure 8(a) and (b) show the historical mean speeds and the actual observed speeds in data respectively. The speeds of road A, B and C marked in Figure 8(b) are very different from those in Figure 8(a). Based on the distinct traffic pattern compared with neighboring roads and the historical average pattern, it is highly possible that these are unreliable speed records caused by sampling bias or peculiar driving behavior. These unreliable speed data will have great impact on common transportation applications.

ST-SCL corrects these unreliable original road speeds, as shown in Figure 8(c). The corrected speeds on roads A and B are more reasonable and have smoother transitions from their adjacent roads. Furthermore, since the length of road C is very short, the speed calculation from trajectories can be unstable, which could result in unreasonable high speeds in both observed and historical mean values. Therefore, ST-SCL gives low confidence for the imputed speed on road C. Comparing Figure 8(c) and (b), ST-SCL provides reliable imputations for the unobserved roads based on the historical pattern and the speeds on adjacent roads. The imputation confidence from ST-SCL also serves as valuable additional information, which could greatly facilitate building more intelligent and robust transportation applications.

7 RELATED WORK

Network-wide traffic state estimation. There are lots of existing works on inferring network-wide traffic states based on various sources of urban sensor data, such as loop detector data [1, 13] and GPS trajectories [20, 21, 24, 28–30]. Many recent studies [20, 22, 31] use graph embeddings or deep graph convolutional networks to model the spatio-temporal dependencies in data for network-wide traffic state estimation . Yi et al. [24] propose a multi-head self-attention based neural network model using trajectory data to infer network-wide traffic speed. Due to data sparsity issue, the temporal resolution of most previous works are around 30 mins to 60 mins, which is too long for fast-changing traffic dynamics in real-world applications. Compared to these works, ST-SCL can adapt to different missing rates of data in a short time slot owing to the SCL strategy, which also allows more robust estimation.

Missing data imputation. Missing data imputation has been studied extensively in the past decades [4, 12, 23]. Most missing data imputation methods [10, 17, 19, 25] focus on building a unified model to infer missing data. As the temporal structure in data are not explicitly captured in these methods, they typically do not provide satisfactory performance for urban data imputation tasks. Some time-series imputation methods are proposed to address this issue, including imitative non-autoregressive model for trajectory imputation [14], using a VAE architecture with Gaussian process to capture temporal dynamics for multivariate time-series imputation [6], and combining long-term temporal dependencies with the representative missing patterns [2]. Nevertheless, some of them are only suitable for single-feature data imputation [5, 14], which are not applicable to model complex spatio-temporal scenarios. In our work, we focus on the network-wide traffic state imputation problem and introduce explicit modeling of the complex spatio-temporal dependencies in data, which provide better model expressiveness and imputation performance.

8 CONCLUSION

In this paper, we propose the ST-SCL framework to solve the network-wide traffic state imputation problem with partially observed, noisy input data from vehicle trajectories. We introduce a novel self-interested coalitional learning (SCL) scheme that can boost the performance of a variety of semi-supervised learning problems by cooperating with an additional discriminator. In our traffic speed imputation problem, ST-SCL leverages a deep learning-based reconstructor to solve the main traffic speed imputation task and a mask discriminative network to facilitate main task learning while providing interpretable confidence measures on the results. The proposed framework incorporates the unique characteristics of the spatio-temporal traffic speed imputation problem while providing robust and interpretable results. The framework is evaluated using a large GPS trajectory dataset from taxis. Extensive experiments against the state-of-the-art baselines demonstrate the effectiveness and robustness of our approach.

9 ACKNOWLEDGMENTS

This work was supported by the National Key R&D Program of China (2019YFB2101805), the National Natural Science Foundation of China (No. 62076191).

REFERENCES

[1] Javed Aslam, Sejoon Lim, Xinghao Pan, and Daniela Rus. 2012. City-scale traffic estimation from a roving sensor network. In *Proceedings of the 10th ACM Conference on Embedded Network Sensor Systems*. 141–154.
[2] Zhengping Che, Sanjay Purushotham, Kyunghyun Cho, David Sontag, and Yan Liu. 2018. Recurrent neural networks for multivariate time series with missing values. *Scientific reports* 8, 1 (2018), 1–12.
[3] Michaël Defferrard, Xavier Bresson, and Pierre Vandergheynst. 2016. Convolutional neural networks on graphs with fast localized spectral filtering. In *Advances in neural information processing systems*. 3844–3852.
[4] A Rogier T Donders, Geert JMG Van Der Heijden, Theo Stijnen, and Karel GM Moons. 2006. A gentle introduction to imputation of missing values. *Journal of clinical epidemiology* 59, 10 (2006), 1087–1091.
[5] William Fedus, Ian J. Goodfellow, and Andrew M. Dai. 2018. MaskGAN: Better Text Generation via Filling in the _______. In *6th International Conference on Learning Representations, ICLR 2018, Vancouver, BC, Canada, April 30 - May 3, 2018, Conference Track Proceedings*.
[6] Vincent Fortuin, Dmitry Baranchuk, Gunnar Rätsch, and Stephan Mandt. 2019. Deep Amortized Variational Inference for Multivariate Time Series Imputation with Latent Gaussian Process Models. (2019).
[7] Ian Goodfellow, Jean Pouget-Abadie, Mehdi Mirza, Bing Xu, David Warde-Farley, Sherjil Ozair, Aaron Courville, and Yoshua Bengio. 2014. Generative adversarial nets. *Advances in neural information processing systems* 27 (2014), 2672–2680.
[8] Patrik O Hoyer. 2004. Non-negative matrix factorization with sparseness constraints. *Journal of machine learning research* 5, 9 (2004).
[9] Diederik P. Kingma and Max Welling. 2014. Auto-Encoding Variational Bayes. In *2nd International Conference on Learning Representations, ICLR 2014, Banff, AB, Canada, April 14-16, 2014, Conference Track Proceedings*.
[10] Yukai Liu, Rose Yu, Stephan Zheng, Eric Zhan, and Yisong Yue. 2019. NAOMI: Non-autoregressive multiresolution sequence imputation. In *Advances in Neural Information Processing Systems*. 11238–11248.
[11] Pierre-Alexandre Mattei and Jes Frellsen. 2019. MIWAE: Deep generative modelling and imputation of incomplete data sets. In *International Conference on Machine Learning*. 4413–4423.
[12] Patrick E McKnight, Katherine M McKnight, Souraya Sidani, and Aurelio Jose Figueredo. 2007. *Missing data: A gentle introduction*. Guilford Press.
[13] Chuishi Meng, Xiuwen Yi, Lu Su, Jing Gao, and Yu Zheng. 2017. City-wide traffic volume inference with loop detector data and taxi trajectories. In *Proceedings of the 25th ACM SIGSPATIAL International Conference on Advances in Geographic Information Systems*. 1–10.
[14] Mengshi Qi, Jie Qin, Yu Wu, and Yi Yang. 2020. Imitative Non-Autoregressive Modeling for Trajectory Forecasting and Imputation. In *Proceedings of the IEEE/CVF Conference on Computer Vision and Pattern Recognition*. 12736–12745.
[15] Xinwu Qian, Xianyuan Zhan, and Satish V Ukkusuri. 2015. Characterizing urban dynamics using large scale taxicab data. In *Engineering and Applied Sciences Optimization*. Springer, 17–32.
[16] Huiling Qin, Xianyuan Zhan, and Yu Zheng. 2021. CSCAD: Correlation Structure-based Collective Anomaly Detection in Complex System. arXiv:2105.14476 [cs.LG]
[17] Trevor W Richardson, Wencheng Wu, Lei Lin, Beilei Xu, and Edgar A Bernal. 2020. MCFlow: Monte Carlo Flow Models for Data Imputation. In *Proceedings of the IEEE/CVF Conference on Computer Vision and Pattern Recognition*. 14205–14214.
[18] Sebastian Ruder. 2017. An overview of multi-task learning in deep neural networks. *arXiv preprint arXiv:1706.05098* (2017).
[19] Marek Śmieja, Łukasz Struski, Jacek Tabor, Bartosz Zieliński, and Przemysław Spurek. 2018. Processing of missing data by neural networks. In *Advances in Neural Information Processing Systems*. 2719–2729.
[20] Xianfeng Tang, Boqing Gong, Yanwei Yu, Huaxiu Yao, Yandong Li, Haiyong Xie, and Xiaoyu Wang. 2019. Joint modeling of dense and incomplete trajectories for citywide traffic volume inference. In *The World Wide Web Conference*. 1806–1817.
[21] Yilun Wang, Yu Zheng, and Yexiang Xue. 2014. Travel time estimation of a path using sparse trajectories. In *Proceedings of the 20th ACM SIGKDD international conference on Knowledge discovery and data mining*. 25–34.
[22] Zonghan Wu, Shirui Pan, Guodong Long, Jing Jiang, Xiaojun Chang, and Chengqi Zhang. 2020. Connecting the dots: Multivariate time series forecasting with graph neural networks. In *Proceedings of the 26th ACM SIGKDD International Conference on Knowledge Discovery & Data Mining*. 753–763.
[23] Junyuan Xie, Linli Xu, and Enhong Chen. 2012. Image denoising and inpainting with deep neural networks. In *Advances in neural information processing systems*. 341–349.
[24] Xiuwen Yi, Zhewen Duan, Ting Li, Tianrui Li, Junbo Zhang, and Yu Zheng. 2019. Citytraffic: Modeling citywide traffic via neural memorization and generalization approach. In *Proceedings of the 28th ACM International Conference on Information and Knowledge Management*. 2665–2671.
[25] Jinsung Yoon, James Jordon, and Mihaela Schaar. 2018. GAIN: Missing Data Imputation using Generative Adversarial Nets. In *International Conference on Machine Learning*. 5689–5698.
[26] Jing Yuan, Yu Zheng, Chengyang Zhang, Xing Xie, and Guang-Zhong Sun. 2010. An interactive-voting based map matching algorithm. In *2010 Eleventh international conference on mobile data management*. IEEE, 43–52.
[27] Bianca Zadrozny, John Langford, and Naoki Abe. 2003. Cost-sensitive learning by cost-proportionate example weighting. In *Third IEEE international conference on data mining*. IEEE, 435–442.
[28] Xianyuan Zhan, Samiul Hasan, Satish V Ukkusuri, and Camille Kamga. 2013. Urban link travel time estimation using large-scale taxi data with partial information. *Transportation Research Part C: Emerging Technologies* 33 (2013), 37–49.
[29] Xianyuan Zhan, Satish V Ukkusuri, and Chao Yang. 2016. A Bayesian mixture model for short-term average link travel time estimation using large-scale limited information trip-based data. *Automation in construction* 72 (2016), 237–246.
[30] Xianyuan Zhan, Yu Zheng, Xiuwen Yi, and Satish V Ukkusuri. 2016. Citywide traffic volume estimation using trajectory data. *IEEE Transactions on Knowledge and Data Engineering* 29, 2 (2016), 272–285.
[31] Ling Zhao, Yujiao Song, Chao Zhang, Yu Liu, Pu Wang, Tao Lin, Min Deng, and Haifeng Li. 2019. T-gcn: A temporal graph convolutional network for traffic prediction. *IEEE Transactions on Intelligent Transportation Systems* 21, 9 (2019), 3848–3858.
[32] Bo Zong, Qi Song, Martin Renqiang Min, Wei Cheng, Cristian Lumezanu, Daeki Cho, and Haifeng Chen. 2018. Deep autoencoding gaussian mixture model for unsupervised anomaly detection. In *International Conference on Learning Representations*.